

NMR evidence for magnetic field confinement of quantum spinons in a weakly coupled $S = 1/2$ spin chain

Long Ma¹, Z. Wang¹, L. Hu^{1,*}, Z. Qu^{1,†}, N. Hao¹, and Li Pi^{1,2‡}

¹ *Anhui Province Key Laboratory of Condensed Matter Physics at Extreme Conditions, High Magnetic Field Laboratory, Chinese Academy of Sciences, Hefei 230031, China*

² *Hefei National Laboratory for Physical Sciences at the Microscale, University of Science and Technology of China, Hefei 230026, China*

(Dated: December 18, 2018)

We report our NMR study of the spin excitations in the quasi-one dimensional (1D) $S = 1/2$ quantum magnet $\text{CH}_3\text{NH}_3\text{Cu}(\text{HCOO})_3$ lying in the 1D-3D dimensional crossover regime. Above T_N , the spinon excitation is observed from the constant $1/T_1$ at low temperatures contributed from the staggered spin susceptibility. At low temperatures well below T_N , free spinons are seen from the flattened out behavior of $1/T_1$ toward zero temperature limit. By the applied field, $1/T_1$ tends to show a power-law temperature dependence gradually, with the index increasing from zero to ~ 3 , and finally ~ 5 , which are the respective typical characteristic for the dominating two-magnon Raman process and three-magnon scattering contributions to the nuclear relaxation in a conventional 3D magnet. This exotic magnetic field tuning of the spin excitations from the quantum spinons to classical magnons implies strong competition between the antiferromagnetic intra-chain interaction and the Zeeman energy.

PACS numbers: 75.10.Pq, 75.40.Gb, 76.60.-k

In low-dimensional (low-D) magnets, the enhanced quantum fluctuations lead to novel states of matter, exotic elementary excitations with integer or fractional quantum numbers, as well as fascinating critical phenomena[1–4]. Studies on the quantum-mechanical effects in low-D magnets have triggered enormous and unending research interest in the condensed matter society, and have profound influence on the understanding of high- T_C superconductivity, fractional quantum Hall effect, and other strongly-correlated electron systems[5–8]. Among others, a prototypical example is the one-dimensional $S = 1/2$ Heisenberg antiferromagnetic spin chain (HAF), where the strong quantum fluctuations prohibit any possible Néel order even at zero temperature limit[9]. This spin system has received long-lived research interest since it's analytically solvable[10], provides a rare opportunity for rigorous comparison between the experimental results and theoretical approach[11, 12], and gives a valuable test of the reliability of the theoretical approximation.

The $S = 1/2$ HAF shows a gapless spin excitation spectrum with a large area of continuum, and the excitation quasiparticle is fractionalized with $S = 1/2$ (spinon)[13, 14]. When the inter-chain coupling is included, long ranged Néel order will be restored at low temperatures, and spinons are bounded to form magnons (spin wave excitation), the Goldstone mode of the symmetry breaking state. By tuning the inter-chain coupling, the dimensional crossover from the critical quantum disordered 1D spin system to the classical 3D magnets occurs, which is important for understanding the semiclassical behavior induced by underlying quantum fluctuations in the materials in the real 3D world.

The quasi-1D HAF is realized in several com-

pounds, KCuF_3 [15–17], Sr_2CuO_3 and SrCuO_2 [18–20], $\text{BaCu}_2\text{Si}_2\text{O}_7$ [21–23] et al. The dimensionality can be measured by the ratio between the intra-chain coupling J and the Néel ordered temperature T_N , also the ordered moment m_0 . For KCuF_3 , $J = 17.5$ meV, $T_N = 39$ K, and $m_0 = 0.5\mu_B$ [15, 16], which is close to the 3D spin system. The more 1D-like character is realized in Sr_2CuO_3 and SrCuO_2 , with a strong intra-chain exchange interaction energy J of ~ 190 meV and ~ 181 meV, a low T_N of 5.4 K and 2 K, and a very small ordered moment both with the order of $< 0.1\mu_B$ (close or below the detecting limit), respectively[18–20]. The $\text{BaCu}_2\text{Si}_2\text{O}_7$ lies on the dimensional crossover regime, where the J equals to 24.1 meV and the antiferromagnetic transition occurs at $T_N = 9.2$ K with a static ordered moment of $0.15\mu_B$ (Refs. [21–23] and therein). According to our knowledge, satisfactory theory described the spin systems near the 1D-3D dimensional crossover region is still highly lacked[24].

Nuclear magnetic resonance (NMR), mainly detecting the on-site hyperfine field and its fluctuations resulting from the electron spins via the hyperfine coupling, is a sensitive local probe for the study of the static magnetism and novel magnetic excitations in the low-dimensional quantum magnet. In this paper, we report our NMR study on the $\text{CH}_3\text{NH}_3\text{Cu}(\text{HCOO})_3$ quantum magnet lying on the 1D-3D crossover regime. Under low magnetic fields, residual free spinon quantum excitation is observed in the Néel ordered state, as evidenced by the nearly temperature-independent $1/T_1$. By increasing the field, the $1/T_1$ gradually shows a power-law temperature dependence at low temperatures with the index of ~ 3 to ~ 5 , corresponding to the two-magnon dominant and three-magnon dominant contributions to the nuclear relaxation in a classical 3D magnet. This result indi-

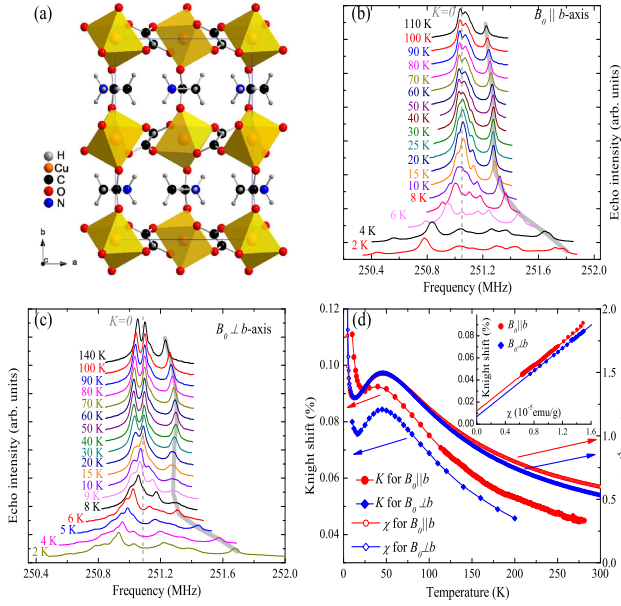


FIG. 1: (color online) (a) The crystal structure of $\text{CH}_3\text{NH}_3\text{Cu}(\text{HCOO})_3$ viewed from c -axis. The chain direction is along the crystalline b -axis, as a result of the much stronger antiferromagnetic coupling. (b) and (c) show typical ^1H NMR spectra under 5.9 T magnetic field with $B_0 \parallel b$ and $B_0 \perp b$ respectively. The gray thick line demonstrates the temperature dependence of the peak position originates from $[\text{HCOO}]^-$ anions. The vertical dashed line shows the Larmor frequency $\gamma_n B_0$. (d) The Knight shift and dc susceptibility versus temperature for both field directions. For the susceptibility measurement, a field of 200 Oe is applied, and the data are collected with the sample warming up after a zero field cooling (ZFC) process. Inset: the Knight shift as a function of dc susceptibility with the temperature as an explicit parameter (See the text).

icates the magnetic field confinement of pairs of quantum spinons into classical 3D magnons in a $S = 1/2$ HAFC system with moderate inter-chain coupling. This newly discovered phenomena should be fresh physical inputs for constructing proper theoretical models.

High quality $\text{CH}_3\text{NH}_3\text{Cu}(\text{HCOO})_3$ single crystals, crystallized in a orthorhombic structure with space group $Pnma$ ($Z = 4$), are synthesized under the solvothermal conditions, as described elsewhere[25]. The intra-chain (along b -axis) coupling J is estimated to be ~ 5.96 meV from dc susceptibility, and the T_N is ~ 4 K at low field[25]. Single crystals with typical dimensions of $2 \times 2 \times 1.5 \text{ mm}^3$ are chosen for our NMR study. Our NMR measurements are conducted on the ^1H nuclei ($\gamma_n = 42.5759 \text{ MHz/T}$, $I = 1/2$) with a phase-coherent NMR spectrometer. The spectra are obtained by summing up the spin-echo intensities as a function of frequency. The spin-lattice relaxation rate is measured by a conventional inversion-recovery method, and fitting the nuclear magnetization to the standard relaxation curve for $I = 1/2$. All the data are collected during a warming-up process

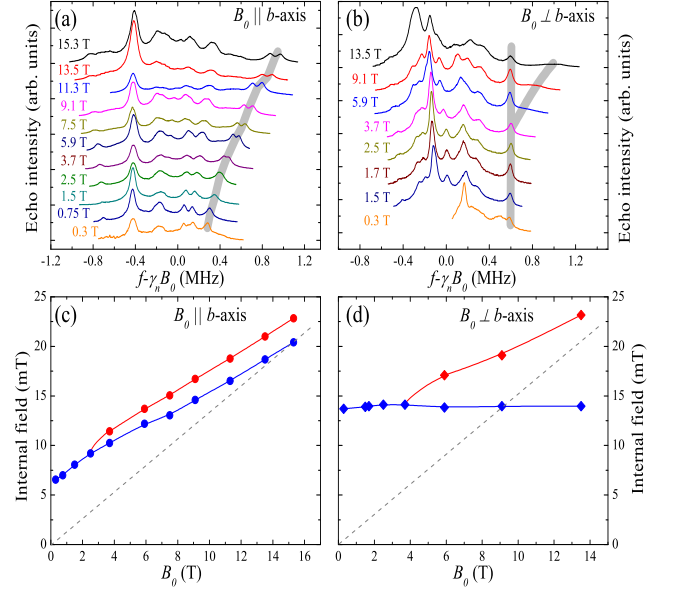


FIG. 2: (color online) The spectra at $T = 2$ K for different field intensities with the $B_0 \parallel b$ (a) and $B_0 \perp b$ -axis (b), respectively. The gray lines show the change of the relative frequency shift of the studied signal peak. (c) and (d): The field dependence of the internal field calculated from $H_{in} = \Delta f / \gamma_n$ of the peaks denoted in (a) and (b) for both directions. The field dependence of the internal field for the paramagnetic state is shown by the dashed line.

for self-consistence.

Typical frequency-swept NMR spectra at various temperatures are shown in Fig.1 (b) and (c) for both field directions. Two groups of signals are clearly identified in the frequency domain. In this magnetic insulator, the hyperfine coupling is mainly contributed from the dipolar interactions between the nuclear spins and electron orbitals and spins, which is very sensitive to the distance between the nuclei and magnetic ions. Thus, we assign the peak at the highest frequency with the largest Knight shift (defined as $K = (f - \gamma_n B_0) / (\gamma_n B_0)$, where the f denotes the actual resonance frequency, and B_0 the applied magnetic field) to the protons from $[\text{HCOO}]^-$ anions, and mainly study the magnetic properties from this site (marked with gray lines). The temperature dependence of the Knight shift in the paramagnetic state is shown in Fig.1 (d), which is consistent with the dc susceptibility. As $K = K_{spin} + K_{orbit} = A_{hf} \chi_{spin} + K_{orbit}$, we can extract the diagonal component of the hyperfine coupling constant tensor A_{hf} from the slope of the line by plotting the Knight shift versus dc susceptibility with temperature as an explicit parameter (See Fig.1(d) inset, also called Clogston-Jaccarino plot[26]). The linear fittings give the hyperfine coupling $A_{hf}^{bb} = 1.254 \text{ kOe}/\mu_B$ and $A_{hf}^{aa/cc} = 1.252 \text{ kOe}/\mu_B$, which is nearly isotropic.

The spectral broadening below $T = 6$ K originates from the emergence of magnetic order. In Fig.2 (a) and

(b), we show the spectra at $T = 2$ K under different fields with $B_0 \parallel b$ and $B_0 \perp b$ -axis. By increasing the field intensity, the spectra are broadened and a slight line splitting for the peak from the $[\text{HCOO}]^-$ anions noted by the gray line is observed for $B_0 > 3.7$ T, which is more clear for $B_0 \parallel b$ (See Fig.2 (a) and (b)). We plot the internal field calculated from the frequency shift $f - \gamma_n B_0$ versus field in Fig.2 (c) and (d). For a line shift and broadening with a paramagnetic origination, the internal field is proportional to the magnetic field, which is shown by the dashed line. However, this is not the actual situation observed in this sample. The field dependence gives an intercept to a nonzero internal field at $B_0 = 0$, which is strong evidence for the magnetically ordered ground state.

The magnetic structure with a G -type antiferromagnetism and a small ferromagnetic component with spin-canting is suggested from the spectra. No line splitting at temperatures below T_N is observed for both field directions, which is different from the ordinary antiferromagnetic order[27]. Two scenarios can be proposed: One is the very small magnetic moment; the other one is the cancelation of the hyperfine field on the ^1H nuclei from the magnetic moments located at the two nearest Cu^{2+} neighbours. By the moderate hyperfine coupling constant discussed above, a $0.06\mu_B$ ordered moment (in Sr_2CuO_3) can result in a line splitting with the frequency distance of ~ 0.64 MHz. In this magnetic insulator lying on the 1D-3D crossover regime, the ordered moment is supposed to be larger than $0.06\mu_B$ as a result of the suppression of quantum fluctuations. Thus, the first scenario is unreasonable, and our results point to the second one.

Every proton in the $[\text{HCOO}]^-$ anions has two nearest Cu^{2+} neighbours along all the three crystalline directions. The cancelation of the internal field occurs only in ordered states with a G -type configuration, where the magnetic moments order antiferromagnetically for all the three directions. The spectrum at $T = 2$ K and its evolution under magnetic field reflect the behavior of the ferromagnetic component of the magnetic order with spin-canting effect along all the three crystalline directions. Based on the Goodenough-Kanamori-Anderson (GKA) rules[28], shorter Cu-Cu distance along b -axis and more significant antiferromagnetic interactions between the half-filled $d_{x^2-y^2}$ through the $[\text{HCOO}]^-$ anions may give much stronger antiferromagnetic coupling along b -axis[25]. The antiferromagnetic coupling between the spin chains is suggested by the mean-field theory[29]. Additionally, the GKA rules also suggest a weak ferromagnetic coupling between spin chains contributed from the coupling between the d_{z^2} orbital and the half-filled $d_{x^2-y^2}$ orbitals. The existing Dzyaloshinskii-Moriya(DM) interactions due to the lack of inversion symmetry along all bond directions lead to the spin-canting along all crystalline directions for the weak ferromagnetic component. These interactions will give rise to the antiferromagnetic

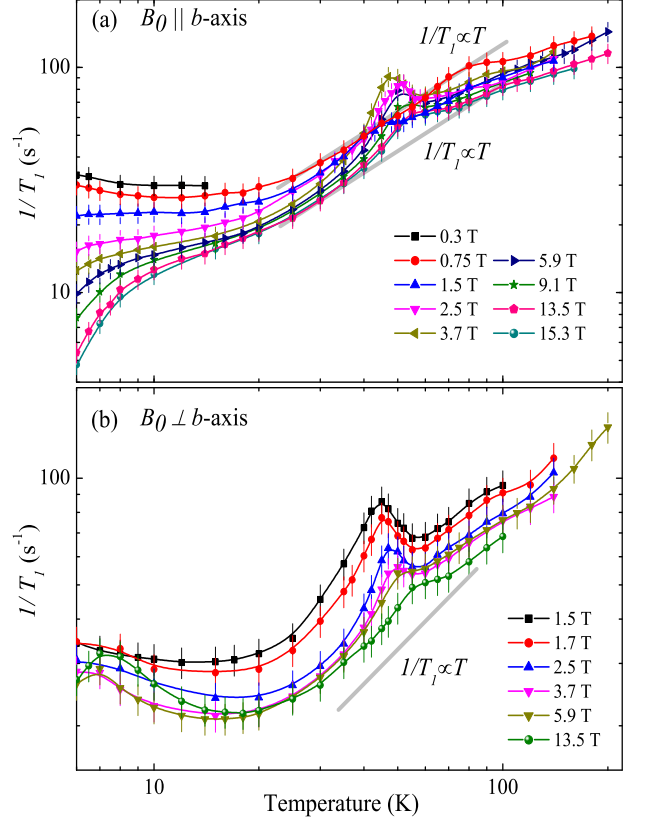


FIG. 3: (color online) The spin-lattice relaxation rate $1/T_1$ in the paramagnetic state ($T \geq 7$ K) as a function of temperature under different field intensities for $B_0 \parallel b$ (a) and $B_0 \perp b$ -axis (b). Solid lines show the linear temperature dependence of $1/T_1$.

order with a G -type configuration and a small ferromagnetic component with spin-canting effect. This is consistent with our spectral analysis on the long-range order below T_N .

Next, we concentrate on the spin excitation and its evolution under the magnetic field. The spin-lattice relaxation rate $1/T_1$ is a measure of the dynamic spin susceptibility, whose temperature and field dependence reveal the nature of the spin fluctuations in the strongly-correlated systems. In Fig.3, we show the temperature dependence of $1/T_1$ above T_N at various magnetic field intensities for both $B_0 \parallel b$ (a) and $B_0 \perp b$ -axis (b). For $B_0 = 0.75$ T $\parallel b$ -axis, the $1/T_1$ shows a nearly temperature-independent behavior from T_N to $T \sim 20$ K, which is followed by the linear temperature dependence denoted by the gray line at higher temperatures. With the field intensity increased, besides the temperature dependence of $1/T_1$ described above, a "hump" structure is observed at temperatures ranged from $T = 40$ K to 60 K. The intensity of the "hump" is enhanced firstly, reaches its maximum at $B_0 = 3.7$ T, and suppressed with further increased field intensity. For $B_0 \perp b$ -axis, similar $1/T_1$

behavior is observed (Fig.3(b)).

The $1/T_1$ behavior shown in Fig.3(a) can be completely understood for this quasi-1D HAFC system. For the applied magnetic field along z direction, the $1/T_1$ can be expressed as

$$1/T_1 = \gamma_n^2 [\langle (\mu_0 h_x)^2 \rangle + \langle (\mu_0 h_y)^2 \rangle] \times \frac{\tau_c}{1 + \omega_L^2 \tau_c^2}$$

, where the the first part before " \times " describes the spin fluctuations at both the directions perpendicular to the applied field[30]. The second part, where τ_c and ω_L denote the typical time scale of the electron system and the nuclear Larmor frequency respectively, undergoes a maximum for $\tau_c = 1/\omega_L$. Thus, we attribute the "hump" structure to the slow dynamics of the spin system.

The scaling theory for the $S = 1/2$ HAFC[31] predicts that the staggered spin susceptibility contributed by spinon excitations dominates the $1/T_1$ at low temperatures ($T \ll J/k_B$), leading to a constant $1/T_1$. While, the uniform spin susceptibility dominating the $1/T_1$ at higher temperatures ($T < J/k_B$), results in a linear temperature dependence of the $1/T_1$. Thus, our data fit quite precisely with this theory, and provide strong evidence for the spinon excitations at low temperatures, and again demonstrate the 1D character of this molecule magnet[32]. This result is obviously very different with the classical spin chains, where the $T^{-3/2}$ temperature dependence of $1/T_1$ is theoretically predicated[33].

The inter-chain coupling results in the 3D Néel order below T_N . In Fig.4 (a) and (b), we show the temperature dependence of $1/T_1$ below T_N for both field directions to study the field dependence of the spin excitations in the ordered state. For $B_0 = 0.3$ T, the nearly-constant $1/T_1$ decreases sharply below T_N , and begins to flatten out below $T \sim 3$ K. With increasing the field intensity, we observe a power-law temperature dependence of the $1/T_1$ for temperatures well below T_N , and further plot the power-law index versus field intensity in Fig.4 (d). For a conventional 3D antiferromagnet, the $1/T_1$ is mainly contributed by the scattering of magnons by nuclear spins. Theoretical calculations[34] predict a T^3 -dependence of $1/T_1$ for the two-magnon Raman process, and a T^5 -dependence of $1/T_1$ for the three-magnon process for $T \gg \Delta$ (Δ is the excitation gap of magnons).

The evolution of the $1/T_1$ under magnetic field can be understood by the confinement of pairs of quantum spinons into classical magnons by magnetic field. This is the first NMR identification of this novel phenomena. The confinement of quasi-particles refers to the physical process that the attracting interaction bounds two quasi-particles with a fractional quantum number to one quasi-particle with an integer quantum number. In the one-dimensional HAFC, a spin-flip ($\uparrow\downarrow\uparrow\downarrow \bullet \uparrow \bullet \uparrow\downarrow\uparrow\downarrow$) costs a energy of intra-chain coupling J , and two "domain walls" (\bullet) are created. However, the diffusion of the "domain wall" ($\uparrow\downarrow \bullet \uparrow\downarrow\uparrow\downarrow \bullet \uparrow\downarrow$) is energy-free. Thus, the

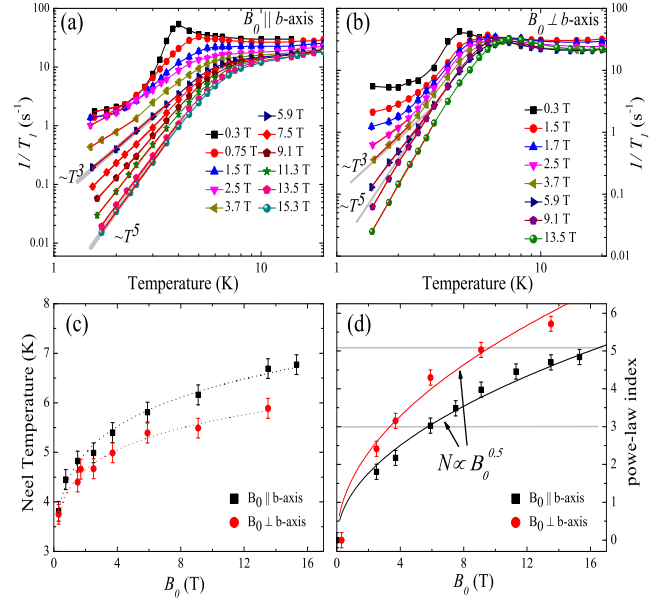


FIG. 4: (color online) The spin-lattice relaxation rate $1/T_1$ below $T = 20$ K, as a function of temperature under different field intensities for $B_0 \parallel b$ (a) and $B_0 \perp b$ -axis (b). Solid lines show the T^3 and T^5 temperature dependence of $1/T_1$. Red straight lines are power-law fits to the $1/T_1$. (c): The field dependence of the Néel temperature. The dotted lines are guides to the eye. (d): The power-law index N as a function of magnetic field. Solid lines are fits to the function $N = A \times \sqrt{B_0}$, where A is the fitting parameter.

first excited state is highly degenerate, and the resulting strong quantum fluctuations prohibit any magnetic orders even at lowest temperatures. For the quasi-1D $S = 1/2$ HAFC system, the inter-chain coupling creates an effective attracting interaction that confines or bounds the pairs of spinons to magnons. Free spinons are observed in KCuF_3 , Sr_2CuO_3 and SrCuO_2 spin systems below T_N by Raman scattering and neutron scattering studies[35, 36]. However, no direct evidence for the magnetic field induced spinon confinement is reported in these compounds.

In the present sample, we see plenty of free spinons in the Néel ordered state, which are further confined into magnons, the quasi-particle of the Goldstone mode in the symmetry-broken state of a classical magnet, by the applied magnetic field with different directions. The increased Néel temperature under magnetic field (See Fig.4 (c)) is also consistent with this suppression of the quantum fluctuations. The inter-chain interaction makes the propagation of spinons consume energy, thus creating an effective attracting potential that confine pairs of spinons. We think the Zeeman energy, proportional to field intensity, should play a similar role. From the spectral analysis, the spin-canting effect induced by the DM interaction is also strongly enhanced under magnetic field, which may be responsible for the crossover from the

dominating two-magnon Raman process to three-magnon scattering contributions to the nuclear relaxation. Up to now, we still don't know the physical origin for the $(B_0)^{0.5}$ field dependence of the power-law index, although this may be important for understanding the confinement. Further theoretical calculation is needed.

To conclude, we have carried out NMR study on a quasi-1D $S = 1/2$ Heisenberg antiferromagnetic chain. The antiferromagnetic long range order is identified from the spectra analysis, and a G -type antiferromagnetism with a ferromagnetic component is proposed. Above T_N , the spinon excitation is observed from the constant $1/T_1$ at low temperatures contributed from the staggered spin susceptibility. At low temperatures well below T_N , free spinons are seen from the flattened out behavior of $1/T_1$ toward zero temperature limit. By the applied field, $1/T_1$ gradually shows a power-law temperature dependence with the index enhanced from zero to ~ 3 , and finally ~ 5 , which are the typical character for the dominating magnon scattering of the nuclear spins in the conventional 3D classical magnet. The result supplies strong evidence for the magnetic field confinement of quantum spinons to classical magnons, which is first reported in the quasi-1D HAFC systems. Additionally, the possible physical origination for the spinon confinement is discussed.

This research was supported by the National Key Research and Development Program of China (Grant No. 2016YFA0401802 and 2017YFA0303201), the National Natural Science Foundation of China (Grants No. 11504377, 11874057, 11574288, U1732273, U1532153, 11774352, 21301178 and 11674331), 100 Talents Programme of Chinese Academy of Sciences (CAS) and the Major Program of Development Foundation of Hefei Center for Physical Science and Technology (Grant No. 2016FXZY001).

* Electronic address: hulin@hmfl.ac.cn

† Electronic address: zhequ@hmfl.ac.cn

‡ Electronic address: pili@ustc.edu.cn

- [1] V. Zapf, M. Jaime, and C. D. Batista, *Rev. Mod. Phys.* **86**, 563 (2014).
- [2] T. Han, J. S. Helton, S. Chu, D. G. Nocera, J. A. Rodriguez-Rivera, C. Broholm, and Y. S. Lee, *Nature (London)* **492**, 406 (2012).
- [3] M. Punk, D. Chowdhury, and S. Sachdev, *Nat. Phys.* **10**, 289 (2014).
- [4] B. D. Piazza, M. Mourigal, N. B. Christensen, G. J. Nilsen, P. Tregenna-Piggott, T. G. Perring, M. Enderle, D. F. McMorrow, D. A. Ivanov, and H. M. Rønnow, *Nat. Phys.* **11**, 62 (2015).
- [5] P. W. Anderson, *Science* **235**, 1196 (1987).
- [6] S. A. Kivelson, D. S. Rokhsar, and J. P. Sethna, *Phys. Rev. B* **35**, 8865 (1987).
- [7] S. Raghu, X.-L. Qi, C. Honerkamp, and S.-C. Zhang, *Phys. Rev. Lett.* **100**, 156401 (2008).
- [8] C. L. Kane and E. J. Mele, *Phys. Rev. Lett.* **95**, 226801 (2005).
- [9] N. D. Mermin and H. Wagner, *Phys. Rev. Lett.* **17**, 1133 (1966).
- [10] H. Bethe, *Z. Phys.* **71**, 205 (1931).
- [11] D. A. Tennant, R. A. Cowley, S. E. Nagler, and A. M. Tsvelik, *Phys. Rev. B* **52**, 13368 (1995).
- [12] P. R. Hammar, M. B. Stone, D. H. Reich, C. Broholm, P. J. Gibson, M. M. Turnbull, C. P. Landee, and M. Oshikawa, *Phys. Rev. B* **59**, 1008 (1999).
- [13] L. D. Faddeev and L. A. Takhtajan, *Phys. Lett. A* **85**, 375 (1981).
- [14] F. D. M. Haldane, *Phys. Rev. Lett.* **66**, 1529 (1991).
- [15] S. K. Satija, J. D. Axe, G. Shirane, H. Yoshizawa, and K. Hirakawa, *Phys. Rev. B* **21**, 2001 (1980).
- [16] M. T. Hutchings, E. J. Samuelsen, G. Shirane, and K. Hirakawa, *Phys. Rev.* **188**, 919 (1969).
- [17] B. Lake, D. A. Tennant, C. D. Frost, and S. E. Nagler, *Nat. Mater.* **4**, 329 (2005).
- [18] K. M. Kojima, Y. Fudamoto, M. Larkin, G. M. Luke, J. Merrin, B. Nachumi, Y. J. Uemura, N. Motoyama, H. Eisaki, S. Uchida, et al., *Phys. Rev. Lett.* **78**, 1787 (1997).
- [19] M. Matsuda, K. Katsumata, K. M. Kojima, M. Larkin, G. M. Luke, J. Merrin, B. Nachumi, Y. J. Uemura, H. Eisaki, N. Motoyama, et al., *Phys. Rev. B* **55**, R11953(R) (1997).
- [20] I. A. Zalitznyak, C. Broholm, M. Kibune, M. Nohara, and H. Takagi, *Phys. Rev. Lett.* **83**, 5370 (1999).
- [21] A. Zheludev, M. Kenzelmann, S. Raymond, E. Ressouche, T. Masuda, K. Kakurai, S. Maslov, I. Tsukada, K. Uchinokura, and A. Wildes, *Phys. Rev. Lett.* **85**, 4799 (2000).
- [22] I. Tsukada, Y. Sasago, K. Uchinokura, A. Zheludev, S. Maslov, G. Shirane, K. Kakurai, and E. Ressouche, *Phys. Rev. B* **60**, 6601 (1999).
- [23] A. Zheludev, K. Kakurai, T. Masuda, K. Uchinokura, and K. Nakajima, *Phys. Rev. Lett.* **89**, 197205 (2002).
- [24] B. Y. Pan, Y. Wang, L. J. Zhang, and S. Y. Li, *Inorg. Chem.* **53**, 3606 (2014).
- [25] B. Pato-Doldán, L. C. Goómez-Aguirre, A. P. Hansen, J. Mira, S. Castro-García, M. Sánchez-Andújar, M. A. Senñaris-Rodríguez, V. S. Zapf, and J. Singleton, *J. Mater. Chem. C* **4**, 11164 (2016).
- [26] A. M. Clogston and V. Jaccarino, *Phys. Rev.* **121**, 1357 (1961).
- [27] L. Ma, J. Dai, P. S. Wang, X. R. Lu, Y. Song, C. L. Zhang, G. T. Tan, P. C. Dai, D. Hu, S. L. Li, et al., *Phys. Rev. B* **90**, 144502 (2014).
- [28] J. B. Goodenough, *Magnetism and the Chemical Bond* (Interscience (Wiley), New York, 1963).
- [29] H. J. Schulz, *Phys. Rev. Lett.* **77**, 2790 (1996).
- [30] C. P. Slichter, *Principles of Magnetic Resonance* (Springer, Berlin, 1990).
- [31] S. Sachdev, *Phys. Rev. B* **50**, 13006 (1994).
- [32] M. Takigawa, N. Motoyama, H. Eisaki, and S. Uchida, *Phys. Rev. Lett.* **76**, 4612 (1996).
- [33] M. E. Fisher, *Am. J. Phys.* **32**, 343 (1964).
- [34] D. Beeman and P. Pincus, *Phys. Rev.* **166**, 359 (1968).
- [35] D. A. Tennant, T. G. Perring, R. A. Cowley, and S. E. Nagler, *Phys. Rev. Lett.* **70**, 4003 (1993).
- [36] O. V. Misochko, S. Tajima, C. Urano, H. Eisaki, and S. Uchida, *Phys. Rev. B* **53**, R14733(R) (1996).